ELSEVIER

Carbohydrate Research 310 (1998) 65–75

CARBOHYDRATE RESEARCH

Complex melting of semi-crystalline chicory (*Cichorium intybus* L.) root inulin

Christophe L.M. Hébette [a,d], Jan A. Delcour [a,*], Michel H.J. Koch [b], Karl Booten [c], Ralf Kleppinger [d], Nikolai Mischenko [d], Harry Reynaers [d]

[a] *Laboratorium voor Levensmiddelenchemie, Katholieke Universiteit Leuven, Faculteit Landbouwkundige en Toegepaste Biologische Wetenschappen, Kardinaal Mercierlaan 92, B-3001 Heverlee, Belgium*

[b] *European Molecular Biology Laboratory, EMBL c/o DESY, Notkestrasse 85, D-22603 Hamburg, Germany*

[c] *Tiense Suikerraffinaderij, Aandorenstraat 1, B-3300 Tienen, Belgium*

[d] *Laboratorium voor Macromoleculaire Structuurchemie, Katholieke Universiteit Leuven, Celestijnenlaan 200F, B-3001 Heverlee, Belgium*

Received 2 February 1998; accepted in revised form 6 June 1998

Abstract

When concentrated solutions (30–45% by weight) of inulin (degree of polymerization 2–66, number average degree of polymerization 12) are cooled at 1 °C/min or 0.25 °C/min from 96 °C to 20 °C, suspensions of semi-crystalline material in water are formed. A thermal nucleation process was detected by optical microscopy: the 8-like shaped crystallites resulting from primary nucleation at higher temperature are larger than those resulting from secondary nucleation at lower temperature. Differential scanning calorimetry (DSC) thermograms display melting profiles with three to four partly overlapping endotherms that vary as a function of concentration, cooling rate during crystallization and storage time at 25 °C of the crystallite suspension. Recrystallization during melting was observed. The wide-angle X-ray scattering patterns of the samples at 25 °C correspond to those of the hydrated crystal polymorph. The structural changes during melting indicated the existence of a single crystal polymorph throughout melting. A periodicity of 95 Å, arising from alternating regions of different electron density, is detected in the small angle X-ray scattering patterns at 25 °C. The stepwise increase of the long period upon heating is related to the existence of two types of lamellar stacks: one with a higher long period, resulting from the primary nucleation and thus crystallized at high temperature, and a second one with a smaller long period, formed by crystallization at lower temperature. The lamellae formed at low temperature melt at a lower temperature than those formed at high temperature, explaining the existence of the two DSC-endotherms.

Keywords: Inulin; chicory root; Fructans; inulin; Polysaccharides; Superstructure

* Corresponding author. Fax: 32 16 321581; e-mail: jan.delcour@agr.kuleuven.ac.be

0008-6215/98/$—see front matter
PII S0008-6215(98)00154-2

1. Introduction

Inulin is a storage polysaccharide found abundantly in the roots of chicory (*Cichorium intybus L.*) and the tubers of dahlia and Jerusalem artichoke. It is a linear fructan consisting of β-(2→1)-linked D-fructofuranose units and one terminal α-(1→2)-linked D-glucopyranose unit. The polydispersity of the molecular chain length depends on the plant species and plants' life cycle [1].

In recent years the food industry has shown a growing interest in inulin. Inulin cannot be directly metabolized by humans[1] [2], and is thus an interesting soluble fiber. It selectively stimulates the growth of Bifidobacteria in the large intestine [3–4], which results in a more healthy intestinal microflora [5,6] as well as in an increase of fecal mass. Finally, the high molecular weight fraction of inulin can replace fat in dietary food products.

Isolation procedures for pure inulin are crucial to guarantee reproducible experimental conditions for analyzing its crystalline behavior. Berghofer et al. [7] used hot water extraction and subsequent crystallization to isolate inulin from sliced chicory roots. Thus, a crude inulin extract was concentrated under reduced pressure to 40 wt% inulin. When the unstirred inulin solution was cooled from 95 to 4 °C over 30 h, part of the inulin precipitated or crystallized as a pasty substance, which could be removed by filtration, and subsequent spray-drying yielded a white powder. Difficulties in processing and removal by filtration of inulin occurred after crystallization [7].

Inulin is an unusually conformationally flexible polysaccharide, since the fructofuranose rings are not part of the polyethyleneoxide-like macromolecular backbone [8–11]. Depending on chain length, several conformations were described in the solid state as well as in solution.

^{1}H NMR experiments [12] showed that in solution *Platycodon grandiflorum* A. DC. inulin oligomers with a degree of polymerization (DP) above eight form a regular five-fold helix. Oligomers with a DP below eight do not adopt this rather rigid secondary conformation. ^{13}C NMR measurements, however, could not confirm such a regular helix for molecular weight fractions with DP between 3 and 9 and for oligomer mixtures with a weight average degree of polymerization (DP_w) 17 of Jerusalem artichoke inulin dissolved in D_2O [13]. For the solid state, Marchessault et al. [10] proposed, based on conformational analysis, X-ray and electron diffraction data, both a left and a right handed five-fold helix for the conformation of inulin in single crystals. In contrast, French [8,9] advocated a six-fold helix on the basis of theoretical considerations. Depending on the hydration conditions, André et al. [11,14] observed two crystalline polymorphs for single crystals of fractionated chicory root inulin with a number average degree of polymerization (DP_n) 17 and a weight average degree of polymerization (DP_w) 20. The difference between the hydrated and the semihydrated polymorph was not ascribed to a conformational change, but solely to a variation in water content. In both polymorphs, the inulin molecule adopts a six-fold helical conformation.

The single crystals in the experiments cited above [10,11,14] were all obtained by slow crystallization from very dilute solutions. The present article describes the complex melting and crystalline behavior of suspensions of inulin crystallites obtained by dynamic and isothermal crystallization from concentrated solutions.

2. Experimental

Materials.—Raftiline ST® and three other inulin powders with different molecular weight (MW) distributions were kindly supplied by the 'Tiense Suikerraffinaderij'. Raftiline ST® is unfractionated, spray-dried inulin (inulin DP 2-66, containing limited quantities of glucose, fructose and sucrose) isolated from the roots of *Cichorium intybus* L. This unfractionated inulin (UI) is polydisperse and has a DP_n 12. The three other inulin powder samples, named intermediate-molecular-weight inulin (IMWI), high-molecular-weight inulin (HMWI) and ultra-high-molecular-weight inulin (UHMWI) were obtained by fractionation of Raftiline ST® and have different MW distributions. Unless indicated otherwise, UI was used for all experiments.

Determination of the polydispersity.—The polydispersity in chain length of inulin was determined qualitatively [15]. The Dionex® series 4500i apparatus was equipped with an eluent degassing module, a Dionex®-pulsed electrochemical detector, a gradient pump, an autosampler and a Shimadzu

[1] I.B. Hesson and K.E.B. Knudsen (1990) Absorption of fructooligosaccharide in the small intestine; M. Robertfroid et al., Private Communication [4].

C-R4AX chromatopac integrator. The injected samples (50 μL, 1% solution) first passed an ion pac (HPIC AG6A; P/N 037141 S/N 2106) pre-column before passing to the analytical CarboPac™ PA-1 column (4×250 mm; P/N 35391 S/N 3963). The bound material was eluted by a NaOH–NaOAc gradient.

Determination of the number average degree of polymerization (DP_n).—The DP_n of the inulin was determined as a fructose to glucose ratio, after complete hydrolysis with SP230 Novozym inulinase for 30 min at 60 °C at pH 4.5; the glucose and fructose concentration before hydrolysis were taken into account [15,16].

Turbidimetry.—A sealed glass tube (length 150 mm, radius 7.5 mm, thickness 1 mm) containing the sample was placed in a glass container heated by a temperature controlled oil bath. A thermocouple was placed in the stirred sample to monitor its temperature. The glass tube was positioned in a laser beam generated by a Spectra Physics Model 133 laser and the transmitted intensity was continuously monitored by a photo cell. This setup allowed continuous monitoring of the transmitted intensity at $2\theta = 0°$ as a function of time and hence, temperature. The onset of turbidity corresponded approximately to 1% of the difference in transmitted intensity between the solution and the fully crystallized sample.

Dynamic crystallization of inulin.—Inulin powder (concentration range between 30 and 45 wt% on a total sample weight of 12 g) was stirred in deionized water and three droplets of 2 M NaOH were added. The suspension was heated in a glass tube (as above) at 96 °C until turbidity measurements in the temperature controlled glass tube indicated that the inulin had completely dissolved. The stirred solution was cooled from 96 to 20 °C and subsequently stored at room temperature. To characterize the thermal history of a sample, zero time was chosen as the moment the cooled solution reached room temperature. Unless otherwise indicated, all dynamically crystallized samples were prepared at a 1 °C/min cooling rate.

Isothermal crystallization of inulin.—Isothermally crystallized samples were obtained by cooling a stirred solution (preparation see above) from 96 °C at 1 °C/min to the isothermal crystallization temperature (65 or 77 °C). After 12 h at 65 or 77 °C the semi-crystalline suspensions were cooled at 1 °C/min to 20 °C and stored at room temperature.

Optical microscopy.—Samples were viewed with an Olympus BH-2 polarization microscope (magnification 500). They were injected in a brass sample holder designed for liquids and placed in a Mettler FP-82 HT oven, and viewed upon cooling at 1 °C/min or heating at 5 °C/min between 20 and 95 °C.

Differential scanning calorimetry.—Differential scanning calorimetry (DSC) was performed using a Perkin–Elmer DSC 7 (cooling device at -30 °C). The instrument was calibrated with indium and benzophenone standards at constant scanning rate (5, 10 or 20 °C/min). Sample pans were Perkin–Elmer type 'large volume capsules for volatile samples.' Every sample was equilibrated 5 min at 10 °C before heating from 10 to 120 °C. All data were normalized based on the sample dry weight content.

Wide angle X-ray scattering (WAXS).—Wide angle X-ray scattering at room temperature was registered on a Rigaku powder diffractometer in the reflection mode using Ni-filtered Cu K_α radiation, generated by a Rigaku-Denki rotating anode device operated at 40 kV and 100 mA, in conjunction with a scintillation counter. The patterns were recorded with a fixed time of 12 s per step of 0.05° in the range $5° \leq 2\theta \leq 60°$.

Time-resolved synchrotron-radiation WAXS and small angle X-ray scattering (SAXS).—Time-resolved synchrotron-radiation WAXS and SAXS patterns during heating were recorded on the X33 double focussing monochromator-mirror camera [17] of the EMBL on the storage ring DORIS III of the Deutsches Elektronen Synchrotron (DESY) in Hamburg, using the standard data acquisition system [18]. Samples with 1.0 mm thickness, packed in a brass sample holder sealed with aluminum foil, were placed in a Mettler FP-82 HT oven through which the X-ray beam passed, and heated from 25 to 103 °C at 2 or 5 °C/min. Simultaneous WAXS and SAXS measurements were recorded as a function of time and hence, temperature. The data were normalized to the incident beam intensity and corrected for detector response. A background corresponding to the amorphous inulin sample was subtracted. Data processing was handled by the OTOKO software package [19].

3. Results and discussion

Characterization of the inulin samples.—The HPAEC-chromatograms of UI, IMWI, HMWI, and UHMWI are presented in Fig. 1. UI, IMWI,

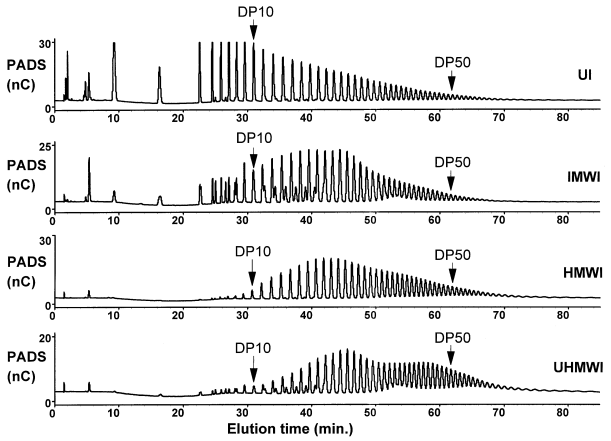

Fig. 1. HPAEC chromatograms of unfractionated inulin (UI), intermediate-molecular-weight inulin (IMWI), high-molecular-weight inulin (HMWI) and ultrahigh-molecular-weight inulin (UHMWI). The elution time (min) increases with the degree of polymerization (DP) of the molecules. The height of the pulsed amperometric detection signal (PADS) in nC of the different peaks in each chromatogram allows a comparison of the molecular weight distribution of the different samples.

HMWI, and UHMWI had DP_n-values of 12, 24.5, 28.5, and 36.5, respectively.

Crystallization.—In the case of dynamic crystallization, the onset of turbidity was detected during the cooling, whereas for isothermal crystallization it occurred during the 12 h isothermal treatment. Optical microscopy revealed a thermal nucleation process consisting of two steps: a first nucleation at higher temperature, yielding 8-like shaped inulin crystallites (Fig. 2), and a second nucleation at lower temperature, also yielding 8-like shaped particles which were ten times smaller than those of the first nucleation. Crystallites from the first nucleation have indeed more time to grow at higher inulin concentration and are also for a certain time growing at higher temperature, where diffusion of molecules to the crystal surface is faster. The thermal nucleation process can partly be attributed to a fractionation of the polydisperse inulin: long chains are less soluble than short chains, and therefore will have a higher effective crystallization temperature. The 8-like shaped inulin crystallites were randomly oriented in the suspension and the larger crystallites (5–20 μm length) were dichroic. Independently of the crystallization procedure, the dense crystallite suspension developed into a gel-like mash over a period of 48 h (for a 30 wt% sample).

DSC-measurements.—Effect of aging on the DSC profiles. DSC measurements (Fig. 3) on a dynamically crystallized 30 wt% sample, homo-

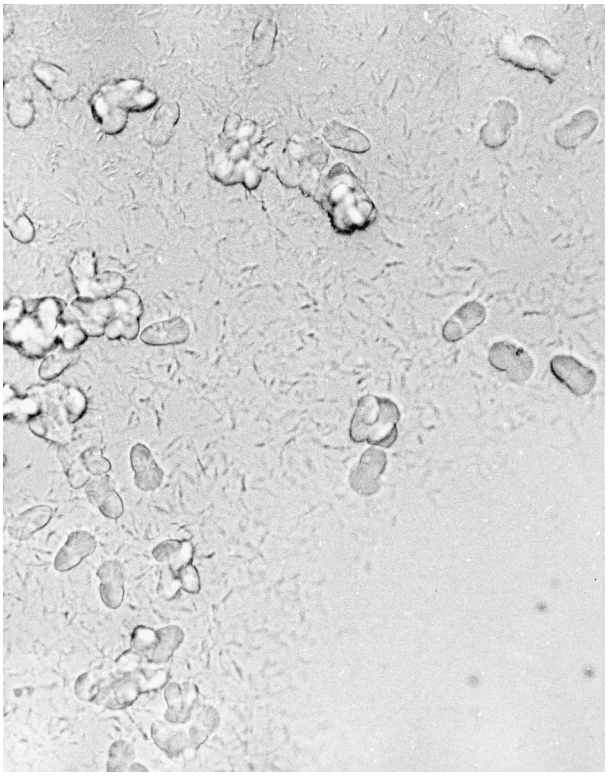

Fig. 2. 8-like shaped inulin crystallites with a length of 10 μm, obtained by dynamic crystallization of a 35 wt% UI solution at 1 °C/min from 96 °C, observed by optical microscopy at magnification 500. The thin small crystallites result from the second nucleation.

genized by stirring, showed that, one hour after reaching room temperature, only two endotherms (referred to as 2 and 4 in Fig. 3) are observed when heating at 5 °C/min from 10 to 120 °C. As time proceeds, two additional endotherms (referred to as 1 and 3 in Fig. 3) clearly develop. The complex melting profile of inulin extends over a temperature range of about 50 °C. No further changes occur in the melting profile after 48 h. DSC traces of isothermally crystallized samples contained two endotherms and revealed the development of a third endotherm similar to endotherm 1 of the dynamically crystallized sample on storage at room temperature. Such changes indicate the formation of additional structures, most probably due to further crystallization during storage at room temperature. These structures have a lower thermal stability than those formed at high temperature.

Effect of concentration on the DSC profiles. Solutions (96 °C) of different inulin concentrations were dynamically crystallized by cooling at 1 °C/min. The resulting crystallite suspensions were kept at room temperature for at least 48 h before DSC analysis, to include the influence of further

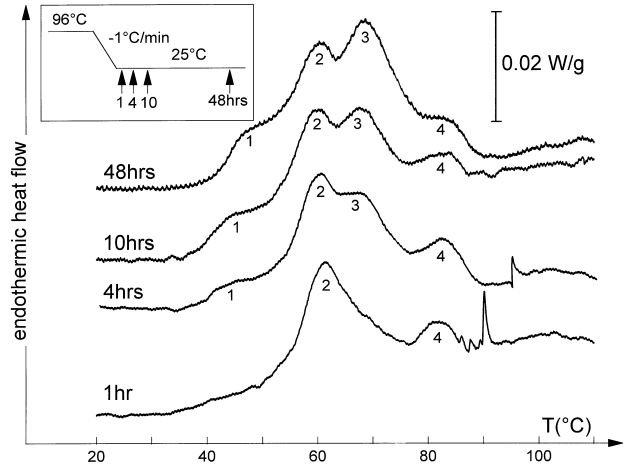

Fig. 3. DSC thermograms recorded upon heating at 5 °C/min from 10 to 120 °C, taken at different times during the storage at room temperature of a 30 wt% unfractionated inulin sample, dynamically crystallized with a cooling rate of 1 °C/min from 96 to 20 °C. For each DSC trace the endothermic heat flow was normalized according to the dry weight of the sample. The different traces were displaced along the ordinate for better visualization. Insert: temperature during dynamic crystallization. The arrows indicate the storage time (h) at room temperature at which the samples for DSC were taken.

crystallization at room temperature (see above). The thermograms in Fig. 4 are all characterized by four endotherms, except for those of the 37 wt% (not shown) and 40 wt% samples, where endotherms 2 and 3 apparently overlap. Endotherms 3 and 4 shift to higher temperatures for increasing inulin concentrations, which is not the case for endotherms 1 and 2.

Effect of the cooling rate during crystallization on the DSC profiles. Two 38.5 wt% inulin suspensions were prepared by dynamic crystallization of solutions at 96 °C, one by cooling at 0.25 °C/min, the other by cooling at 1 °C/min. Turbidity was detected at 68.5 °C and 52 °C, respectively. Both crystallite suspensions were kept at room temperature for at least 48 h before DSC analysis. The cooling rate during crystallization significantly influences the melting behavior of the resulting suspensions (Fig. 5). Endotherm 3 has a higher melting temperature and melting enthalpy when the sample is cooled at 0.25 °C/min than at 1 °C/min, whereas the melting enthalpy of endotherm 4 is lower when cooling at 0.25 °C/min than at 1 °C/min. The change in positions of endotherms 1 and 2 is small. Similar observations were made for 35 and 45.7 wt% samples.

Effect of molecular weight distribution on the crystallization and the DSC-profiles. Two series (30 and 35 wt%) of four samples with different MW distribution (UI, IMWI, HMWI, and UHMWI, see Fig. 1) were dynamically crystallized by cooling at 1 °C/min from 96 °C to room temperature. Turbidimetry indicates that, at equal concentrations, samples with a high-fraction of high-molecular-weight inulin crystallize after a shorter time and at a higher temperature than the samples with a high fraction of low-molecular-weight inulin (see Table 1). Although suspensions of 30 wt% of UHMWI in water at 96 °C became less turbid, they did not fully solubilize even after 2 h at 96 °C. The DSC thermograms of the crystal suspension in Fig. 6 illustrate that the highest temperature endotherm shifts to higher temperatures with increasing proportion of high-molecular-weight polymers.

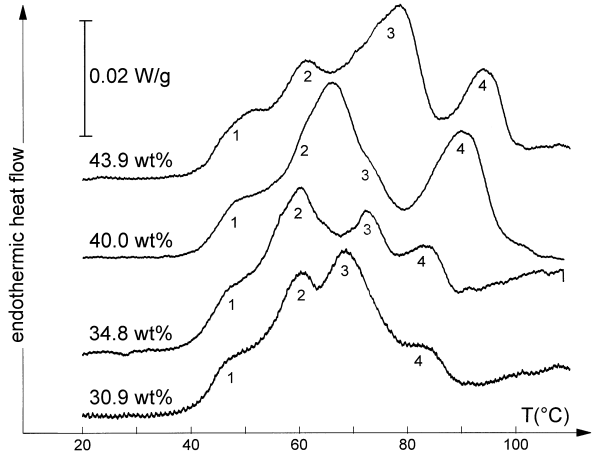

Fig. 4. DSC thermograms, recorded at 5 °C/min from 10 to 120 °C, 48 h after dynamic crystallization by cooling at 1 °C/min from 96 °C to room temperature of solutions with different concentration of unfractionated inulin.

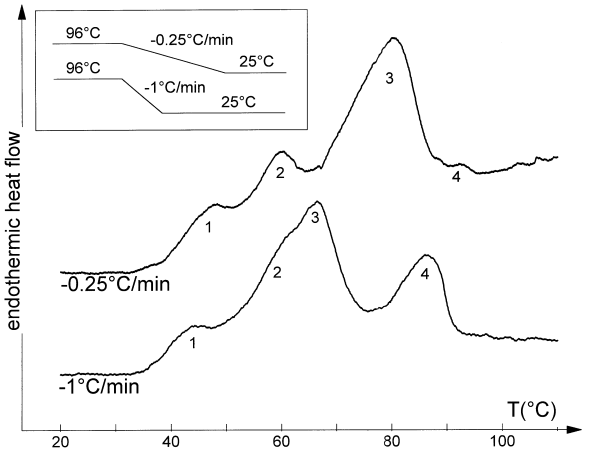

Fig. 5. DSC thermograms, recorded at 5 °C/min from 10 to 120 °C, of 38.5 wt% samples of unfractionated inulin, dynamically crystallized at 1 °C/min and 0.25 °C/min. Insert: cooling profiles during dynamic crystallization at 1 and 0.25 °C/min.

Table 1
Temperatures at which the onset of crystallization (T_{cr}) is detected by turbidimetry for samples with different molecular-weight distributions [UI, IMWI, HMWI, UHMWI (see Fig. 1)] at 30 and 35 wt%, when cooled from 96 to 25 °C at 1 °C/min

Sample	T_{cr}(30 wt%) (°C)	T_{cr}(35 wt%) (°C)
UI	29	42
IMWI	28	42
HMWI	41	64.5
UHMWI	—[a]	—[a]

[a] not fully soluble at 96 °C.

HPAEC on each individual type of crystallite, separated by centrifugation during crystallization from concentrated solutions of UI, indicated cocrystallization of low-molecular-weight material in high-molecular-weight inulin crystals and vice versa. The above data point to a partial fractionation during crystallization, resulting in crystallites with a high relative concentration of high-molecular-weight inulin, and crystallites enriched in low-molecular-weight inulin.

Comparison of the melting behavior of dynamically and isothermally crystallized samples. In contrast with the DSC thermograms of dynamically crystallized samples, which all display four endotherms, those of isothermally crystallized samples of identical concentration (30–45 wt%) only exhibit three endotherms after 48 h. The position of the lower temperature endotherms in Fig. 7 is approximately the same for the dynamically and isothermally crystallized samples. Endotherm C

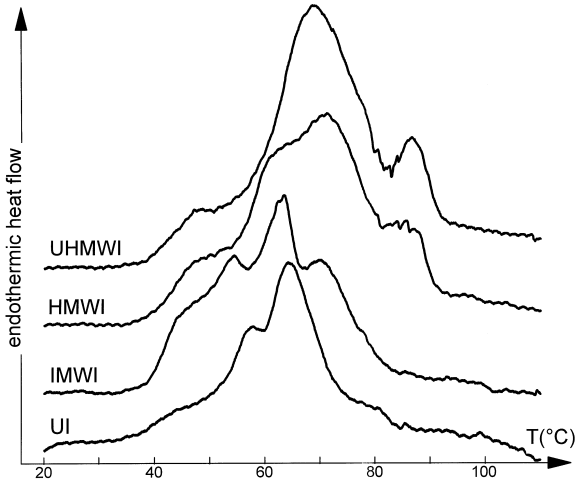

Fig. 6. DSC thermograms, recorded at 5 °C/min from 10 to 120 °C, of 30 wt% inulin samples with different molecular-weight distribution [unfractionated inulin, IMWI, HMWI, and UHMWI (see Fig. 1)], 48 h after dynamic crystallization at 1 °C/min.

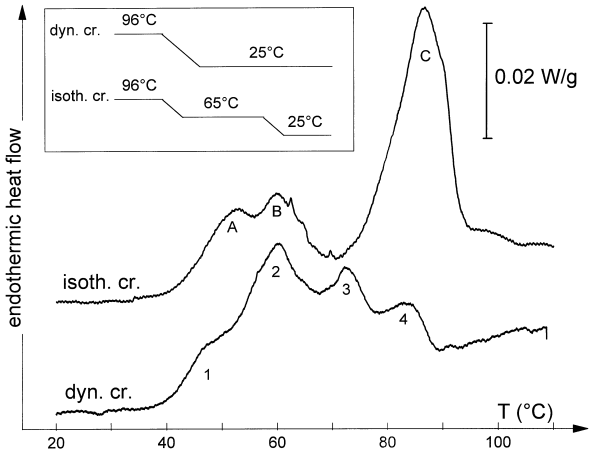

Fig. 7. DSC thermograms of 35 wt% samples of unfractionated inulin, recorded at 5 °C/min from 10 to 120 °C, of a sample isothermally crystallized at 65 °C and a sample dynamically crystallized at a cooling rate of 1 °C/min. Insert: Cooling profiles during dynamic and isothermal crystallization.

shifts to higher temperatures when the sample is isothermally crystallized at higher temperature. The melting enthalpy of the highest temperature endotherm is much higher for isothermally crystallized samples than for the dynamically crystallized ones. Endotherm 3 of the dynamically crystallized sample is absent in the isothermally (65 and 77 °C) crystallized samples, although peak overlap as in Fig. 4 is not to be excluded. Multiple runs with identical 45 wt% samples suggest that the sum of the estimated enthalpies corresponding to endotherms 3 and 4 in a dynamically crystallized sample is comparable with the melting enthalpy of endotherm C of the same sample crystallized isothermally at 77 °C. When assuming a comparable specific enthalpy for endotherms 3 and 4, a tentative explanation is that during dynamic crystallization the residence time of the sample in the high temperature range is restricted and therefore only a part of the high-molecular-weight (HMW) fraction molecules will crystallize at a higher temperature. Hence, crystallization occurs at lower temperature, yielding thinner and less perfect lamellar crystals [20]. It is reasonable to expect that, under isothermal crystallization conditions, the HMW fraction crystallizes almost completely at high temperature, while the temperature is too high for the low-molecular-weight fraction to crystallize. During and after cooling the crystallite suspension from 77 °C to room temperature, there is additional crystallization of the low-molecular-weight fraction. Due to the smooth polydispersity, some

intermediate chain lengths may crystallize over a broad temperature range, depending on crystallization time and temperature. Co-crystallization of a limited amount of low-molecular-weight material with high-molecular-weight material can also not be excluded.

Recrystallization during melting. Dynamically (1 °C/min) and isothermally (77 °C) crystallized samples of equal concentrations (45 wt%) were heated in the DSC at 5, 10 and 20 °C/min. The enthalpy change in endotherm 4 of the dynamically crystallized samples in Fig. 8 decreases with higher scanning rates, indicating recrystallization. The thermograms of the 45 wt% isothermally crystallized samples (Fig. 9) display a clear recrystallization exotherm between 60 and 85 °C, which is most pronounced at a scanning rate of 20 °C/min. This exotherm is absent in the dynamically crystallized samples, where it is probably masked by endotherm 3. The position of the exotherm suggests that the recrystallization is related to the material responsible for endotherms 1 and/or 2. Since, as illustrated in Fig. 3, only endotherms 2 and 4 occur one hour after reaching room temperature, endotherm 4 is, at least partly, due to recrystallization of the material of endotherm 2. Further evidence for such recrystallization stems from the lower melting enthalpy of endotherm 4 material on Fig. 5 when cooling at the lower cooling rate. It is obvious that in dynamically crystallized samples with high concentrations and in isothermally

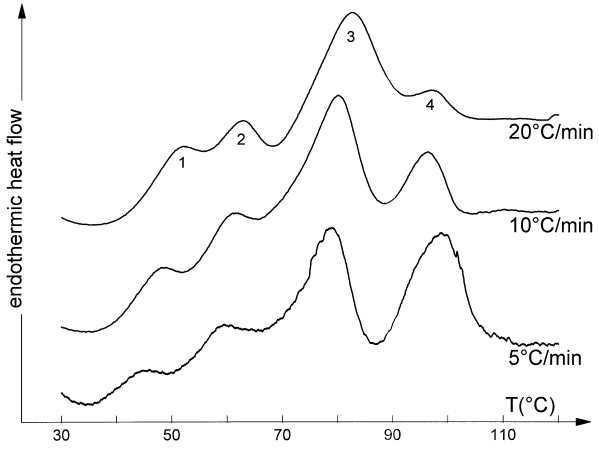

Fig. 8. DSC thermograms of a 45 wt% sample of unfractionated inulin, dynamically crystallized with a cooling rate of 1 °C/min recorded at respectively 5, 10 and 20 °C/min. To facilitate a qualitative comparison of the traces, their different slopes are set to 0 and the endothermal scale is adapted for each DSC thermogram individually. Therefore comparisons can only be made between endotherms of each individual DSC thermogram.

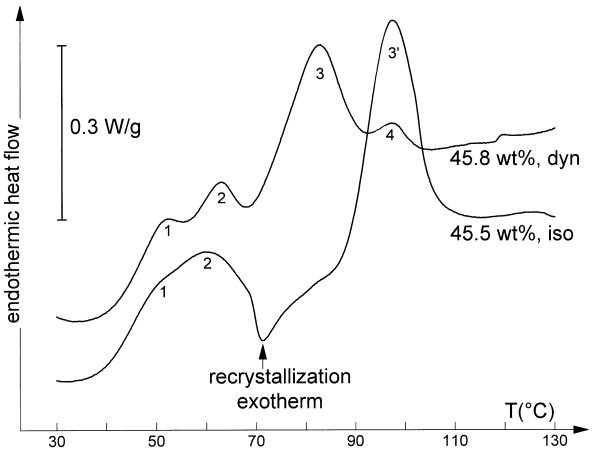

Fig. 9. Comparison of DSC thermograms, recorded at 20 °C/min, of two 45wt% unfractionated inulin samples, one isothermally crystallized at 77 °C and the other dynamically crystallized with a cooling rate of 1 °C/min, both taken after 48 h storage at room temperature.

crystallized samples the formation of the material involved in endotherm 4 already partly takes place at high temperature during the crystallization period. This, of course, does not exclude the recrystallization of the material involved in endotherm 2 upon heating at a later stage. The above fail, however, to explain the formation of endotherm 3 material, which, in spite of being formed at room temperature, is of higher thermal stability than the endotherm 1 and 2 material in Fig. 3. Recrystallization of endotherm 1 material into endotherm 3 material would imply a dependence of the melting enthalpy on the scanning rate, which is not the case, as illustrated in Fig. 8. Apparently, the process is more complicated, probably due to the melting of endotherm 2 material (HMW) that takes place simultaneously with a possible recrystallization of endotherm 1 material (LMW). This might result in interdiffusion of low- and high-molecular-weight chains, giving rise to structures with a melting point in between endotherm 2 and 4.

X-ray scattering.—Wide angle X-ray scattering. WAXS-patterns were obtained at room temperature for a 1 °C/min dynamically crystallized 45 wt% sample and for a 45 wt% sample isothermally crystallized at 77 °C. The numerous peaks in the diffraction patterns (see Table 2) confirm the crystalline nature of inulin [7,10,14]. The positions of the peak maxima in the two scattering curves are approximately identical, although there may be slight changes in the relative intensities of the reflections. The d-values and the relative

Table 2
Comparison of the d-spacings and their related intensities obtained from the experimental WAXS diffraction maxima of suspensions of unfractionated inulin with the d-spacings and their related intensities of the hydrated and semi-hydrated inulin polymorph given by André et al. [11]. The fast dynamical crystallization yields less perfect crystals and hence less well resolved reflections

At 1 °C/min dynamically crystallized 45 wt% sample		Hydrated polymorph (André et al.)		Semi-hydrated polymorph (André et al.)	
d-spacing (Å)	Relative intensity	d-spacing (Å)	Relative intensity	d-spacing (Å)	Relative intensity
11.043	40	11.15	weak	11.29	weak
7.279	91	7.41	very strong	8.32	very strong
5.417	21	5.45	very weak	7.21	very strong
4.993	76	5.01	strong	5.49	medium
4.679	26	4.64	weak	4.87	very strong
4.055	100	4.2	strong	4.55	medium
3.675	55	3.7	weak	4.2	medium

intensities of all samples closely match those of the hydrated inulin polymorph [11,14]. Concentrations from 30 up to 45 wt% yielded diffractograms with identical d-values.

Time-resolved WAXS measurements using synchrotron radiation. A dynamically crystallized sample (45 wt%) was heated at 5 °C/min from 25 to 103 °C. Above 40 °C, a smooth decrease in scattered intensity as a function of temperature is observed, indicating a progressive loss of crystallinity as illustrated in Fig. 10. At 80 °C, the reflection at a d-spacing 7.2 Å is very weak, pointing to some residual crystallinity. Above 80 °C, the sample becomes more fluid and its WAXS pattern is essentially featureless. Melting at 5 °C/min does not proceed over semihydrated forms and thus the different endotherms in the DSC thermogram, recorded at 5 °C/min, are solely related to thermal effects in the hydrated polymorph [11,14].

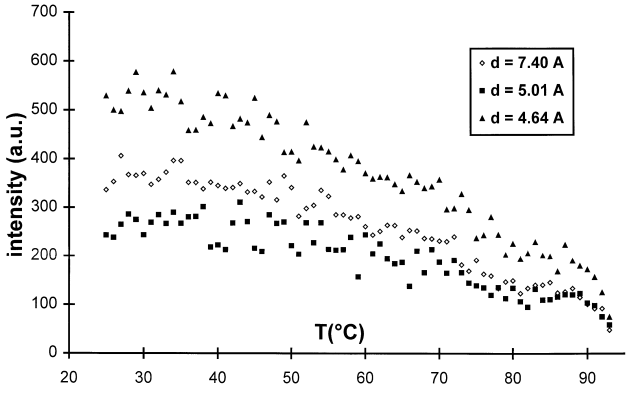

Fig. 10. Decrease in intensity of the peak maxima of the three strongest wide-angle scattering peaks for a dynamically crystallized 45 wt% unfractionated inulin sample upon heating at 5 °C/min from 25 to 103 °C. Peak 1 corresponds to d = 7.4 Å, peak 2 to d = 5.01 Å and peak 3 to d = 4.64 Å.

Time-resolved SAXS measurements using synchrotron radiation. SAXS measurements during the crystallization of a 40 wt% solution upon cooling from 96 to 25 °C at 1 °C/min revealed the formation of a superstructure with a long period of 110 Å at higher temperature, followed by a decrease of the long period down to 98 Å upon further cooling to room temperature. When an identical 40 wt% solution was cooled at 20 °C/min from 96 to 25 °C only the formation of a superstructure with a long period of 90 Å was detected.

Single crystals of inulin, crystallized from dilute solutions, have a lamellar character [10,11,14] and it thus seems justified to attempt an interpretation of the SAXS patterns, obtained during crystallization of concentrated solutions, in terms of a two phase model consisting of stacks of lamellar crystals, separated by amorphous regions. Electron micrographs confirm the presence of stacks of lamellar crystals in frozen samples, crystallized from concentrated solutions (unpublished results).

From the results above, it was concluded that the 40 wt% sample cooled down at 1 °C/min consists of two populations of lamellar stacks: one with a long period of 110 Å formed at high temperature, and another with a long period of 90 Å formed at lower temperature, yielding an average long period of 98 Å, depending on the ratio of both populations. The sample cooled at 20 °C/min did not have the time to crystallize at high temperature and thus consisted only of one population of stacks formed at low temperature. This hypothesis is supported by optical microscopy observations during crystallization, where the formation of 8-like shaped crystallites at high temperature probably corresponds to the superstructure with a long

period of 110 Å, whereas the formation of the smaller crystallites at lower temperature is related to the formation of superstructures with a long period of 90 Å.

SAXS also reveals the presence of periodic superstructures in both the dynamically and isothermally crystallized 45 wt% samples. The position of the maximum, observed at room temperature in synchrotron SAXS-scattering curves of dynamically crystallized samples, corresponds to a periodicity of 95 Å. Upon heating at 5 °C/min, this spacing increases in a quasi-stepwise manner between 40 and 80 °C as illustrated in Fig. 11. This stepwise increase in long period is related to the melting of lamellar stacks formed at low temperature, while the lamellar stacks formed at high temperature are thermostable. The small depression in the long period around 65 °C coincides with the temperature domain in which, according to DSC experiments, recrystallization takes place. A recrystallization may very well lead to the formation of new lamellae nucleated by the thermostable particles, resulting in an overall decrease in long period (new lamellae growing in between the thermostable lamellar stacks).

The suspension consists of three phases: the solution, the crystalline lamellae and the amorphous material between the lamellae. By substracting the solution scattering from the total scattering, one ends up with the scattering from the amorphous and crystalline phase. For such a two phase system, the invariant Q is given by:

$$Q = 4\pi \int s^2 I(s) \mathrm{d}s = K(\rho_c - \rho_a)^2 \varphi(1-\varphi)$$

with $|s| = \frac{2\sin\vartheta}{\lambda}$, the modulus of the scattering vector s and 2ϑ the scattering angle, ρ_c the electron density of the lamellar crystals, ρ_a the electron density of the amorphous material in between adjacent lamellae, φ and $(1-\varphi)$ respectively, the volume fractions of the crystalline and amorphous phases and K a constant containing information on the type of interaction, experimental and sample characteristics. As all measurements were done on a relative scale and were normalized to the intensity of the incident beam, the discussion is limited to changes in the electron density difference between the two phases and to changes in volume fraction of the components. Above 40 °C, Q decreases continuously, indicating a decrease of $\varphi(1-\varphi)$ resulting from the melting of crystalline lamellae, as confirmed by the progressive intensity decrease in the WAXS pattern. The decrease of Q coincides with the first traces of melting, observed by DSC. This evidences that the melting of structural entities dominates a possible influence of the mosaicity of the crystalline lamellae when the 45 wt% sample is heated at 5 °C/min.

At 80 °C, a superstructure, as evidenced by the periodicity, is no longer detectable, although both small and wide-angle diffraction show a weak scattering, most probably related to individual small crystals of high thermal stability (see Figs. 11 and 12). On further heating the invariant

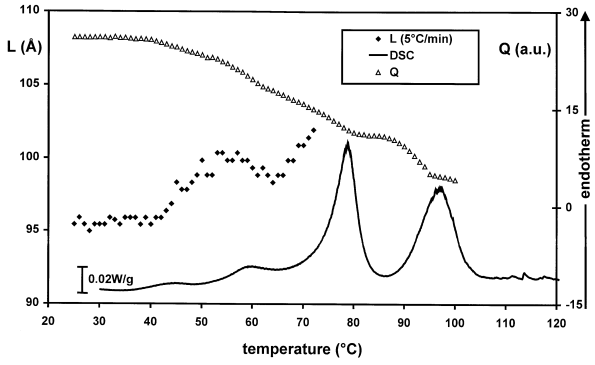

Fig. 11. Evolution of the invariant Q and the long period L (Å), calculated from the maxima in the SAXS-scattering curves, upon dynamic heating at 5 °C/min from 25 to 103 °C of a 45 wt% unfractionated inulin sample. The DSC thermogram of an identical sample heated at 5 °C/min from 20 to 130 °C was integrated in the picture in order to visualize the relation between superstructure and melting behavior. The bottom trace is the DSC thermogram of the same sample recorded at 5 °C/min.

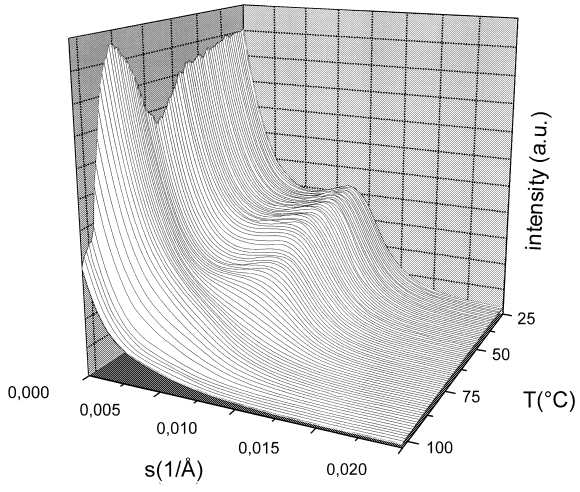

Fig. 12. Evolution of the SAXS pattern as a 45 wt% unfractionated inulin sample is heated from 25 to 103 °C at 5 °C/min. The intensity in arbitrary units was plotted versus the s-value (s = scattering vector) and temperature.

Q continues to decrease, suggesting the melting of the residual crystals, until the typical scattering pattern of a polymer solution is obtained (see Fig. 12). Microscopy experiments on at 1 °C/min dynamically crystallized 45 wt% samples, heated at 5 °C/min from 20 to 95 °C, revealed a sample that was non-transparent upto 85 °C. Between 85 and 95 °C a suspension of slowly melting, needle-like 8-shaped structures was observed.

These observations confirm the conclusions drawn from the SAXS and WAXS data below 80 °C. The melting observed above 80 °C in the DSC traces probably pertains to highly stable semi-crystalline lamellae no longer available in stacks.

4. Conclusions

Dynamic cooling at 1 °C/min of a solution of unfractionated inulin at 96 °C results in an aqueous suspension of inulin crystallites. The crystallization process is initiated by thermal nucleation. Part of the inulin crystallizes at higher temperatures, yielding 8-like shaped particles that, at the end of crystallization, are about ten times larger than the part crystallized at lower temperature. These two nucleation steps shift to higher temperatures with increasing inulin concentrations. DSC reveals complex melting behavior of such a crystallite suspension. The DSC melting endotherms that were detected right after reaching 25 °C were related to the first nucleation and crystal growth at higher temperature, whereas the endotherms that appeared as a function of storage time at 25 °C were related to the second nucleation and crystal growth at 25 °C. The inverse relation between the degree of undercooling during crystallization and the melting temperature of the crystals explains the two lower temperature endotherms. Changes in cooling rate during crystallization and initial inulin concentration affect the melting behavior of the crystal suspension since they change both the temperature at which the first nucleation occurs, and the rate and time for crystal growth at higher temperatures.

It is proposed that fractionation occurs during crystallization as the longer chains have a lower solubility than the shorter ones and therefore crystallize more rapidly and also at higher temperatures during dynamic crystallization. The fractionation effect is however not very sharp: part of the low-molecular-weight material cocrystallizes with high-molecular-weight material in the crystals at higher temperature. Diffusion of high-molecular-weight chains to the crystal surface is relatively slow and the material not incorporated in the high temperature crystals contributes with low-molecular-weight material to the formation of crystals at room temperature.

DSC measurements at different scanning rates indicate that the material involved in endotherm 2 recrystallizes upon heating into endotherm 4 material.

WAXS of an isothermally crystallized sample and a dynamically crystallized sample shows that both samples point to the hydrated crystal polymorph described by André et al. [11]. Time-resolved WAXS-data indicate that the crystallinity in dynamically crystallized samples decreases slowly upon heating, without the selective disappearance of any diffraction maximum.

Time-resolved SAXS data during dynamic crystallization of a 40 wt% sample reveal two populations of periodic superstructures with an average long spacing of about 98 Å. The first population has a long period of 110 Å in the lamellar stacks and is related to crystal growth at higher temperature, whereas the second population has a long period of 90 Å and is related to crystal growth at lower temperatures. The degree of undercooling during crystallization is inversely related with the thickness and perfection of the crystalline lamellae and their melting temperature. When a fully dynamically crystallized 40 or 45 wt% sample is heated the average long period slightly but systematically increases, and the lamellar stacks crystallized at low temperature melt first, followed by the melting of lamellar stacks crystallized at higher temperature. Upon further heating the superstructure transforms in a suspension of individual crystals as manifested by particle scattering, and near the end of melting solution scattering is observed. Around 65 °C a decrease in long period, related to recrystallization of endotherm 2 material, was detected.

The complex melting behavior of inulin depends on several parameters, which all affect the crystallization temperature and the relative rates of crystallization of chains of different molecular weight at a given temperature. Fractionation of UI is now needed in order to explore the influence of the molecular weight on the crystallization and melting behavior.

Acknowledgements

This work was carried out with the support of the European Union through the HCMP Access to Large Installation Project; contract no. CHGE-CT93-0040.

References

[1] L. De Leenheer and H. Hoebregs, *Starch/Staerke*, 46 (1994) 193–196.
[2] U. Nilsson, R. Oste, M. Jagerstad, and D. Birkhed, *J. Nutr.*, 118 (1988) 1325–1330.
[3] X. Wang and G.R.Gibson, *J. Appl. Bacteriol.*, 75 (1993) 373–380.
[4] M. Robertfroid, G.R. Gibson, and N. Delzenne, *Nutr. Rev.*, 51 (1993) 137–146.
[5] T. Mizutani, I. Benno, and T. Mitsuoka, *Nutr. Rep. Int.*, 26 (1982) 279–289.
[6] J.L. Rasic, *North Eur. Dairy J.*, 4 (1983) 80–88.
[7] E. Berghofer, A. Cramer, V. Schmidt, and M. Veigl, *Pilot-scale Production of Inulin from Chicory Roots and its Use in Foodstuffs*, in A. Fuchs (Ed.), *Inulin and Inulin-containing Crops*, 1st ed., Elsevier Science, Amsterdam, 1993, pp 77–84.
[8] A.D. French, *Plant Physiol.*, 134 (1989) 125–136.
[9] A.D. French, *Recent Advances in the Structural Chemistry of Inulin*, in A. Fuchs (Ed.), *Inulin and Inulin-containing Crops*, 1st ed., Elsevier Science, Amsterdam, 1993, pp 121–127.
[10] R.H. Marchessault, T. Bleha, Y. Deslandes, and J.F. Revol, *Can. J. Chem.*, 58 (1980) 2415–2422.
[11] I. André, J.-L. Putaux, H. Chanzy, F.R. Taravel, J.W. Timmermans, and D. de Wit, *Int. J. Biol. Macromol.*, 18 (1996) 195–204.
[12] M. Oka, N. Ota, Y. Mino, T. Iwashita, and H. Komura, *Chem. Pharm. Bull.*, 40 (1992) 1203–1207.
[13] J. Liu, A.L. Waterhouse, and N.J. Chatterton, *J. Carbohydr. Chem.*, 13 (1994) 859–872.
[14] I. André, K. Mazeau, I. Tvaroska, J.-L. Putaux, F.R.Taravel, W.T. Winter, and H. Chanzy, *Macromolecules*, 29 (1996) 4626–4635.
[15] J. Van Loo, P. Coussement, L. De Leenheer, H. Hoebregs, and G. Smits, *Crit. Rev. Food Sci. Nutr.*, 35 (1995) 525–552.
[16] J.W. Timmermans, M.B. van Leeuwen, H. Tournois, D. de Wit, and J.F.G. Vliegenthart, *J. Carbohydr. Chem.*, 13 (1994) 881–888.
[17] M.H.J. Koch and J. Bordas, *Nucl. Instrum. Methods Phys. Res.*, 208 (1983) 461–469.
[18] C.J. Boulin, R. Kempf, A. Gabriel, and M.H.J. Koch, *Nucl. Instrum. Methods Phys. Res. Sec. A*, 269 (1988) 312.
[19] C.J. Boulin, R. Kempf, M.H.J. Koch, and S.M. Mc Laughlin, *Nucl. Instrum. Methods Phys. Res. Sec. A*, 249 (1986) 399–407.
[20] B. Wunderlich (Ed.), *Macromolecular Physics, Vol. 2, Crystal Nucleation, Growth, Annealing*, 1st Ed., Academic Press, New York, 1976, pp 83–85.